UDC 617-7
DOI: 10.15587/1729-4061.2026.363988

CONSTRUCTION OF A TWO-PHASE MODEL FOR HEATING BIOLOGICAL TISSUE AND ELECTROSURGICAL INSTRUMENTS WITH A SPLIT ELECTRODE

Alexei Lebedev
Corresponding author
Doctor of Technical Sciences, Professor*
E-mail: biowelding@gmail.com
ORCID: https://orcid.org/0000-0002-8692-6677
Vladyslav Shlykov
Doctor of Technical Sciences, Professor*
ORCID: https://orcid.org/0000-0001-8836-4658
Andrii Dubko
Candidate of Technical Sciences, Associate Professor*
Department of Welding and Related Technologies in Medicine and Ecology
E. O. Paton Electric Welding Institute
Kazimierz Malevich str., 11, Kyiv, Ukraine, 03150
ORCID: https://orcid.org/0000-0001-6070-3945
Stanislav Popov
PhD Student*
ORCID: https://orcid.org/0000-0003-1518-6824
*Department of Biomedical Engineering
Igor Sikorsky Kyiv Polytechnic University
Beresteysky ave., 37, Kyiv, Ukraine, 03056

This study develops a two-phase model for heating biological tissue and electrosurgical instruments with a split electrode in the ANSYS program (USA). The distribution of voltage, temperature in the tissue and instruments depending on time and the thickness of the dielectric between the electrodes has been obtained. The dependences of the coagulation area of the parenchyma on the distance between the electrodes and voltage have been determined.

At a dielectric thickness of 3 mm, the tissue is heated to a maximum temperature of 100°C near the ends of the electrodes. Between the electrodes, the temperature decreases to 80–89°C. Coagulation of the tissue begins at a normal temperature of about 80°C. The coagulation zone has a semicircular shape with a width of 6–7 mm and a maximum depth of about 1–1.5 mm.

The resulting model makes it possible to determine the optimal thickness of the dielectric, voltage, and speed of movement of the instrument depending on the diameter of the electrodes and the properties of the tissue. For an electrode diameter of 6 mm, the optimal dielectric thickness is 2–3 mm, voltage – 20–30 V, average speed of movement – 20–30 mm/s. The greatest depth of coagulation and speed of movement of the tool can be obtained at an insulating washer thickness of 3 mm. If the hemostasis zone is within the surgeon's visibility, s/he manually adjusts the voltage and speed of movement of the tool. If the hemostasis zone is hidden from the surgeon, it is necessary to use automatic control systems.

The results are used for the design of electrosurgical tools and technologies

Keywords: electrosurgery, welding of living tissues, hemostasis, electrosurgical instruments, split electrode, ANSYS

Received 17.03.2026
Received in revised form 26.05.2026
Accepted 05.06.2026
Published 23.06.2026

How to Cite: *Lebedev, A., Shlykov, V., Dubko, A., Popov, S. (2026). Construction of a two-phase model for heating biological tissue and electrosurgical instruments with a split electrode. Eastern-European Journal of Enterprise Technologies, 3 (5 (141)), 36–43. https://doi.org/10.15587/1729-4061.2026.363988*

1. Introduction

In the early 1990s, a technique for welding living tissues was devised at the E. O. Paton Electric Welding Institute. The technique makes it possible to connect biological tissues without threads and clips due to molecular structural changes that occur during electric welding of soft biological tissues. Underlying this theory is the fact that the key role in such a connection belongs to the interaction of collagen structures that form a mesh [1].

More than 150 surgical procedures have been mastered in such fields as general and abdominal surgery [2], traumatology, pulmonology, proctology, urology, mammalogy, otorhinolaryngology [3], and gynecology. In ophthalmology, the detached retina of the eye is fixed to its choroid [4, 5] and tumor resection is performed [6], etc.

Experimental studies on connecting tissues of the small intestine of rats using electric welding are reported in work [7]. The results of histological studies on vascular connections obtained by electric welding are described in [8]. The authors of [9, 10] analyzed the impedance of biological tissues during electric welding. According to surgeons, this process is very promising for the transplantation of various organs. The technology is used in microsurgery. The effectiveness of the welded connection of the nerve is at least not lower than that of suturing the damaged nerve with a microsurgical suture (neurorrhaphy); the dynamics of recovery after operations are quite comparable [11]. The connection is much simpler and does not require exceptionally high qualifications of the surgeon; in the case of operations on nerves in humans, the corresponding surgical intervention will take less time and be less expensive.

Welding is used in neurosurgery for hermetically sealing the dura mater [12, 13] and during the resection of frontal sinus tumors [14]. Electrofusion welding provides an advantage in tensile strength and hermeticity of the electrofusion joint, compared with a joint using suture material. There is minimal traumatic damage to the adjacent dura mater tissue and minimal thermal damage. In some cases, it is not possible to connect the electrode to one side of the tissue being welded. In this case, the electrodes are applied to one side of the tissue. Such instruments are termed split electrode instruments.

The clinical application of live tissue welding is constantly expanding and improving. Therefore, it is a relevant task to study physical processes during the passage of current through a two-phase medium (biological tissue – split electrode).

2. Literature review and problem statement

The patent and research results for a tool with a split electrode for stopping bleeding in the gastrointestinal tract are reported in [15, 16], but there is no information about the temperature regimes of operation of this tool. In work [17], a joint application of optical and mathematical methods is considered for determining the temperature of the tissue. The object of welding is within the operator's visibility. This method cannot be used when stopping bleeding in wound channels where the tool covers the visibility of the coagulation zone.

In [18], an instrument for eliminating bleeding in injuries of parenchymal organs is described. The tool facilitates the work of surgeons, reduces the time of operations, and accelerates the recovery of patients. The tool is designed to stop bleeding on flat surfaces, not in cylindrical channels. In work [19], an electrosurgical instrument for stopping bleeding in places invisible to the surgeon is described. It has the shape of a ring made of insulating material that is worn on the surgeon's finger. During the operation to remove prostate adenoma, the surgeon puts the instrument on his/her finger and alternately "removes" all the nodes of the adenoma with simultaneous hemostasis. The instrument was tested in surgical urological practice and received a positive result. The shape and dimensions of the instrument are not suitable for working in the gunshot wound canal.

In [20], a more convenient form of the instrument with an elongated cylindrical handle for the treatment of chronic tonsillitis was proposed. In this case, the quality of operations significantly improved, namely blood loss during tonsillectomy was reduced by 5.3 times; the duration of the surgical intervention was reduced by 2.1 times; however, no information about the temperature is provided. The instrument with a split electrode is used to treat pathological formations on the surface of the lungs. It makes it possible to seal the lung tissue without overheating and damage. This procedure is easily performed using video thoracoscopy. Conventional devices for wound closure are not required [21].

The papers above provide information about various designs of the instrument with a split electrode and its application in medicine. However, they lack information about electrical and thermal processes, which are very important in the construction of the instrument and the technologies of its application.

The above allows us to argue about the expediency of defining the features of the physical processes that occur when using an electrosurgical instrument with a split electrode.

3. The aim and objectives of the study

The aim of research is to build a two-phase model of heating biological tissue and electrosurgical instruments with a split electrode. This could make it possible:

– to accelerate the surgery and reduce blood loss;

– to improve and accelerate designing the instrument and technologies for its application.

To achieve the goal, the following tasks were set:

– to determine the shape and dimensions of the coagulation area of biological tissue;

– to find the optimal parameters of the instrument and the speed of its movement.

4. The study materials and methods

The object of our study is the operation of an electrosurgical instrument with a split electrode.

The principal hypothesis assumes that determining the physical processes could allow us to speed up the surgery and reduce blood loss.

We adopted the constancy of the parameters of biological tissue and that coagulation depends only on temperature, and not on temperature and time. The simplification was that the influence of the skin effect on the displacement of current to the surface of the electrodes was not taken into account.

When heating biological tissues with a high-frequency current, it is necessary to solve the thermal and electromagnetic problems. To solve the heat transfer problem, first of all, it is necessary to solve the electromagnetic problem and as a result find Q – the distribution function of heating sources. Equation (1) follows from Maxwell's equations [22]: it describes electromagnetic processes in conducting media

$$-\nabla\left(\frac{1}{\mu}\nabla E\right)+\left(j\omega\sigma-\omega^2\varepsilon\right)E=0, \qquad (1)$$

where ∇ is the nabla operator; E is the electric field strength; μ is the magnetic permeability of the conducting medium; j is the imaginary unit; ω is the angular frequency; σ is the specific electrical conductivity; ε is the dielectric constant of the conducting medium.

Equation (1) captures the electric field strength E and the distribution of heating sources Q when a high-frequency current flows in conducting media

$$Q=\sigma E^2. \qquad (2)$$

Temperature distribution in any material is described by the thermal conductivity equation (3), which takes the following form

$$\rho C\frac{\partial T}{\partial t}-\nabla\left(k\nabla T\right)=Q, \qquad (3)$$

where ρ is the density, C is the specific heat capacity; k is the thermal conductivity coefficient; Q is the distribution function of heating sources; T is the temperature.

Maxwell's equations in the ANSYS software environment were solved using the finite element method. The area of the studied object was divided into a finite number of elements. The starting point for the calculations of the electric field strength E and temperature T are differential equations (1) to (3). At each step of the solution, after the electromagnetic analysis, a non-stationary thermal analysis was performed.

5. Results of investigating the heating of biological tissue and electrosurgical instruments with a split electrode

5. 1. Determining the shape and size of the coagulation area of biological tissue

The shape and size of the coagulation area of biological tissue depend on the temperature, which is found by simulation in ANSYS (USA).

The working part of the instrument consisted of two cylindrical electrodes, which are made of copper-molybdenum alloys, and the dielectric – of high-strength plastic. The characteristics of the copper-molybdenum alloy were taken as for ordinary copper (Fig. 1).

To study the heating of the parenchyma model without taking into account large vessels, a biological tissue model was built. The hole from the gunshot wound and the diameter of the electrodes are 6 mm. The length of the parenchyma model is 30 mm, the diameter is 15 mm. The model did not take into account large blood vessels and bronchi (Fig. 2).

The properties of the parenchyma are taken from the biological materials library built into the COMSOL simulation program.

1) density – 1330 kg/m^3;
2) isotropic thermal conductivity – 0.39 W /(m×°C);
3) specific heat capacity at constant pressure – 500 J×kg×°C;
4) isotropic resistivity – 0.107 Ohm/m.

Initial temperature – 36.6°C.

The study involved electrical and temperature analyses. The simulation was performed for electrical voltages of 20, 25, and 30V (Fig. 3, 4). The voltage was applied to the right electrode. The potential of the left electrode was 0. The grid size in this and other figures is 1 * 1 mm

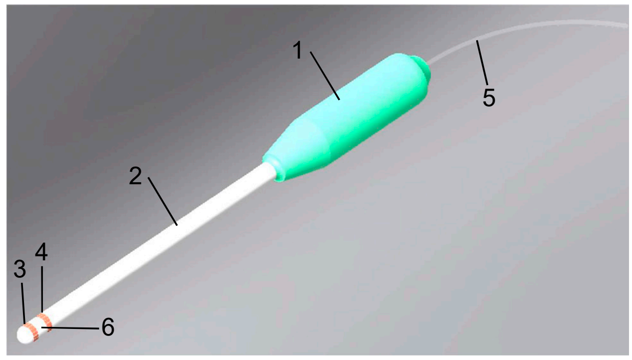

Fig. 1. Split-electrode instrument: 1 — handle; 2 — tube; 3 — electrode; 4 — electrode; 5 — voltage supply cable to the electrodes; 6 — dielectric washer between the electrodes

The distribution of Joule heat density and temperature is shown in Fig. 5, 6. Joule heat is the specific power released when an electric current passes through a tissue.

Fig. 7 shows plots of changes (constructed in Excel (USA)) in the maximum, minimum, and average temperatures.

An approximation of the change in a maximum temperature was determined by a polynomial expression

$$\text{Tmax} = -141.47t^2 + 331.45t + 57.258. \quad (4)$$

Using expression (4), a heating duration of 0.3 s was determined, which prevents excessive overheating of the tissue. Fig. 8, 9 show temperatures for a heating duration of 0.3 s.

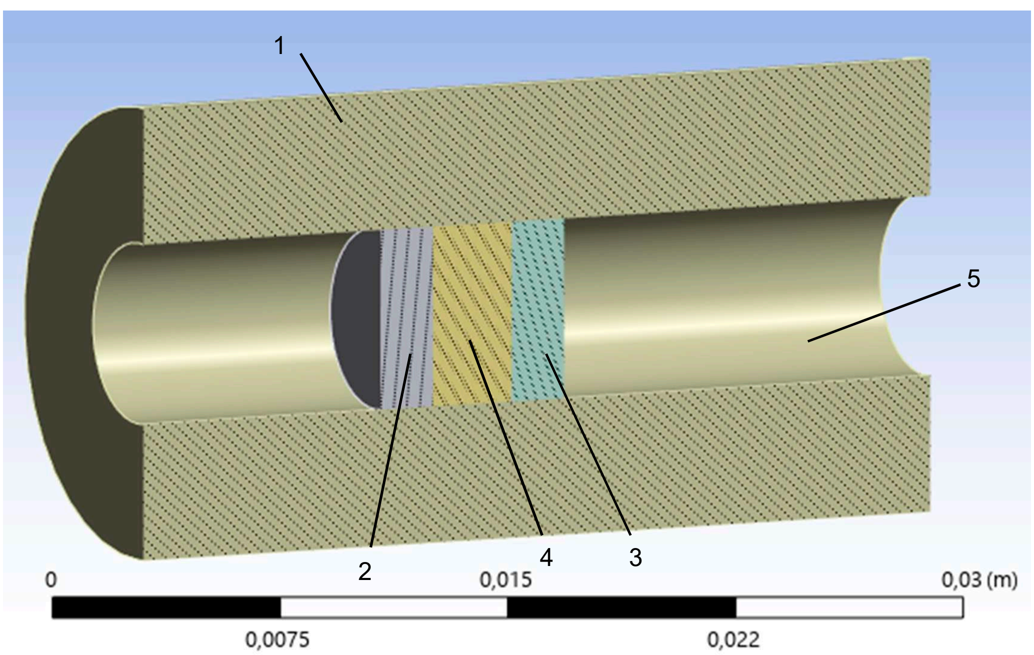

Fig. 2. Biological tissue model: 1 — lung tissue; 2 — electrode; 3 — electrode; 4 — dielectric washer; 5 — gunshot wound channel

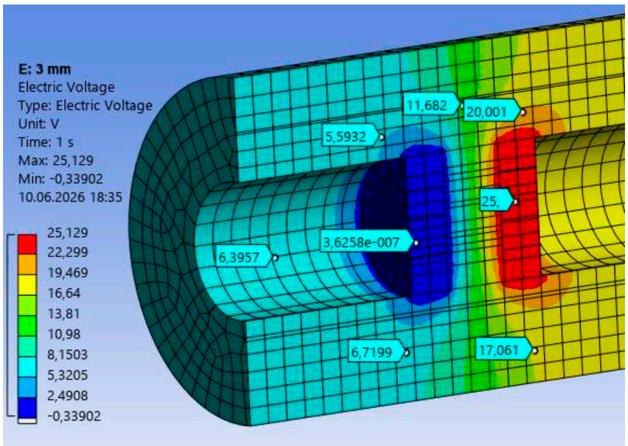

Fig. 3. Voltage distribution of 25V in the parenchyma with a dielectric thickness of 3 mm

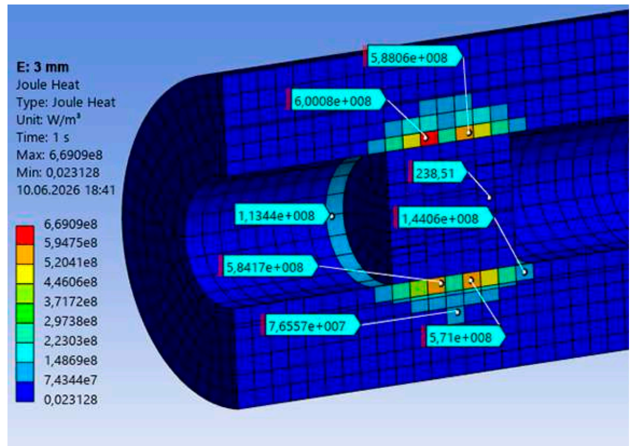

Fig. 5. Distribution of Joule heat release density at a dielectric thickness of 3 mm, voltage of 25 V, and duration of 1 s

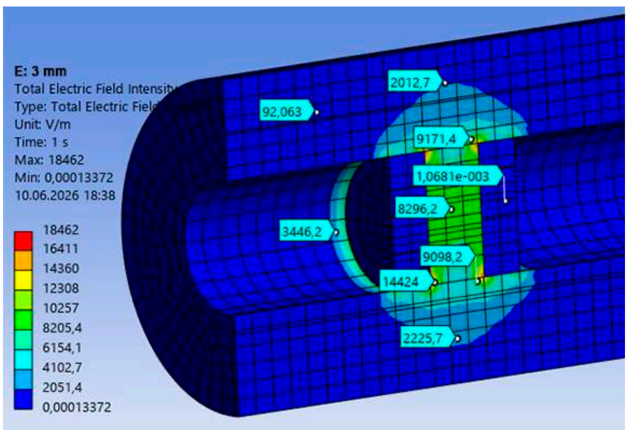

Fig. 4. Voltage gradient distribution at a dielectric thickness of 3 mm and voltage of 25V

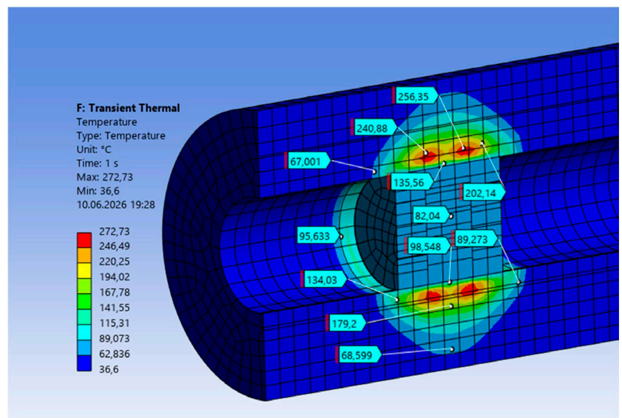

Fig. 6. Temperature distribution at a dielectric thickness of 3 mm, a voltage of 25 V, and a duration of 1 s

Coagulation of tissue begins at a normal temperature of about 80°C. Therefore, the coagulation zone will have a semicircular shape with a width of 6–7 mm and a maximum depth of about 1–1.5 mm.

The dependence of hemostasis depth on voltage was investigated at a dielectric thickness of 3 mm and a duration of 0.3 s (Fig. 10).

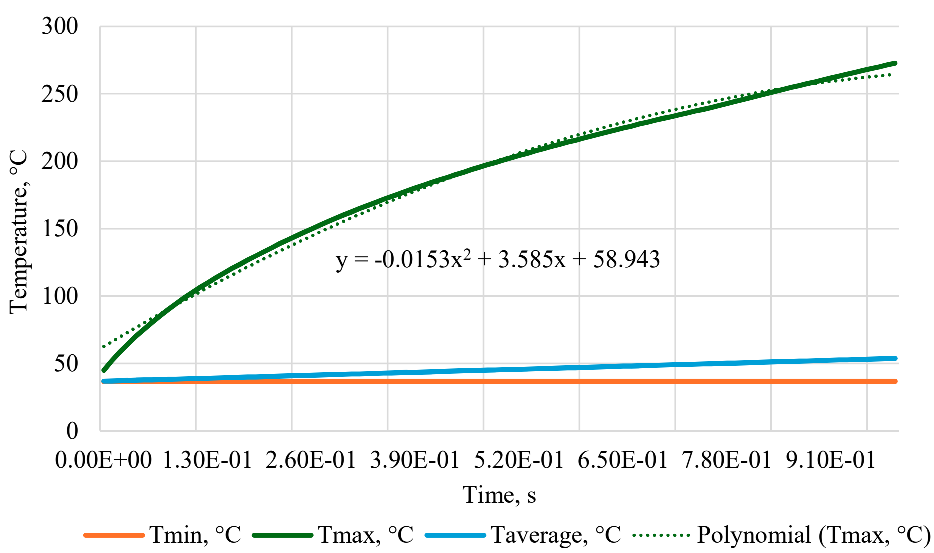

Fig. 7. Changes in the maximum, minimum, and average temperature at a voltage of 25V and a duration of 1 s

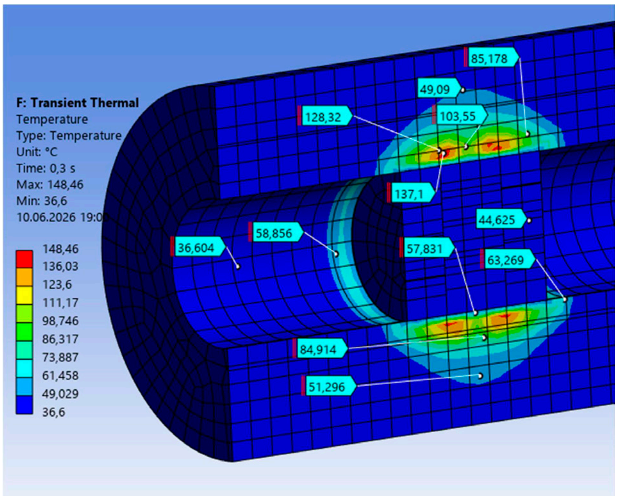

Fig. 8. Temperature distribution at a dielectric thickness of 3 mm, a voltage of 25 V, and a duration of 0.3 s

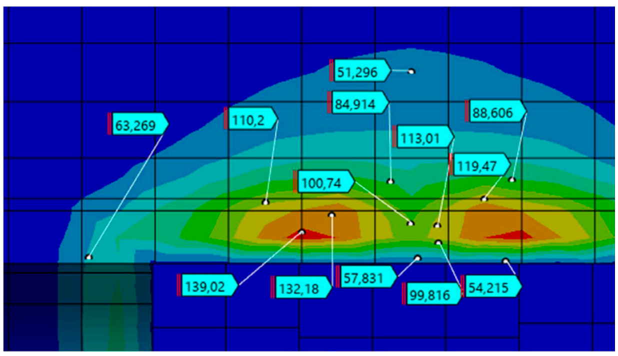

Fig. 9. Enlarged view of half of the hemostasis zone at a dielectric thickness of 3 mm, a voltage of 25 V, and a duration of 0.3 s

The dependence of the depth was also investigated at dielectric thick-nesses of 2, 4, and 5 mm (Fig. 11, 12).

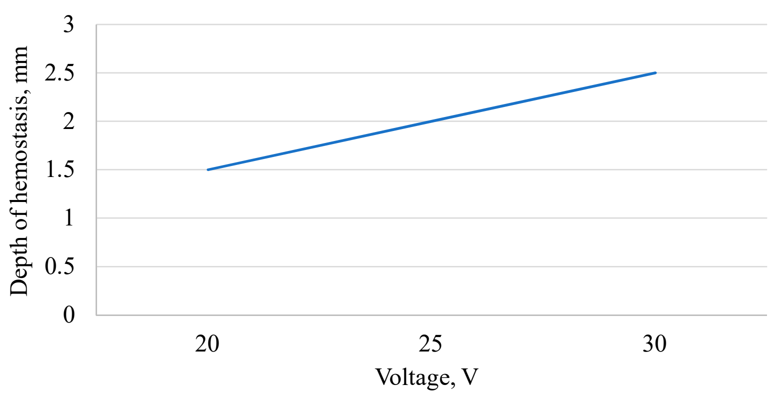

Fig. 10. Dependence of the depth of hemostasis on voltage at a dielectric thickness of 3 mm and a duration of 0.3 s

The maximum hemostasis width of 9.7 mm is achieved with a dielectric thickness of 4 mm and a voltage of 30 V. At the same time, the hemostasis depth of 2.5 mm is close to the maximum. The minimum hemostasis depth of 0.8 mm and its width are achieved with a dielectric thickness of 2 mm and a voltage of 20 V. An increase in voltage at a constant duration of 0.3 s causes an increase in the width of the hemostasis zone and its depth.

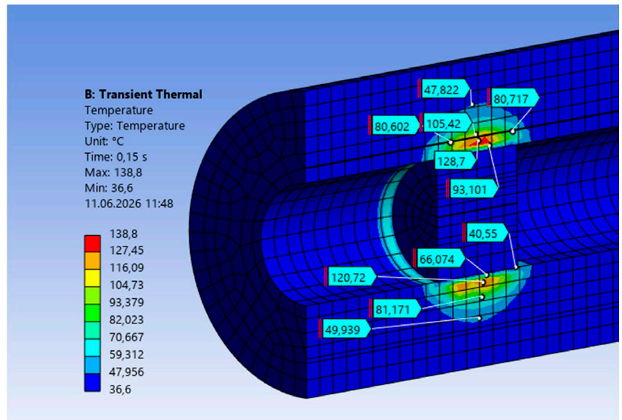

Fig. 11. Temperature distribution at a dielectric thickness of 2 mm, a voltage of 25 V, and a duration of 0.15 s

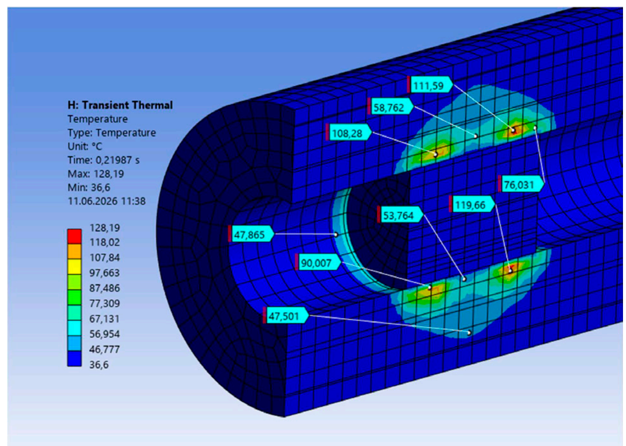

Fig. 12. Temperature distribution at a dielectric thickness of 5 mm, a voltage of 30 V, and a duration of 0.3 s

5. 2. Determining the optimal parameters of the instrument and its movement speed

With a dielectric thickness of 3 mm, the tissue is heated to a maximum temperature of 147°C near the ends of the electrodes (Fig. 8, 9). Areas of elevated temperature occupy a small area of the coagulation zone. Between the electrodes, the temperature decreases to 80–100°C. Let us introduce a temperature non-uniformity coefficient equal to the maximum temperature of 136°C divided by the minimum temperature of 104°C on the line connecting the areas with the maximum temperature. The temperature non-uniformity coefficient is 1.3. In order to avoid tissue overheating, it is necessary to move the tool by 7 mm after 0.3 s. Therefore, the average speed of movement of the instrument will be 7/0.3 = 23 mm/s.

At a dielectric thickness of 2 mm, the zone of maximum temperature is located between the electrodes at all voltages (Fig. 11). Therefore, the coefficient of uneven temperature distribution is 1. To prevent excessive heating, the time was reduced to 0.15 s.

With a dielectric thickness of 4 mm, the zones of maximum temperature are located at the inner ends of the electrodes. The tissue opposite the middle of the insulating plate heats up less. At a voltage of 25 V and a duration of 0.3 s, the temperature in the middle is 71°C with a maximum temperature of 122°C. The coefficient of uneven temperature distribution is 1.71. In order to have hemostasis in the middle zone between the plates, it is necessary to increase the voltage to 35 V. In this case, the temperature in the middle zone increases to 102°C, and the maximum temperature is 201°C. The coefficient of uneven temperature distribution is 1.99. With such a coefficient of unevenness, hemostasis will be uneven.

At a dielectric thickness of 5 mm, the voltage was increased to 30 V to increase the temperature (Fig. 12). The zones of maximum temperature of 130°C are located near the inner ends of the electrodes. The distance between the electrodes is large, so the temperature of 70°C in the middle between them is insufficient for hemostasis. The coefficient of uneven temperature distribution is 1.9. To achieve the required temperature, it is necessary to increase the welding time or voltage. To increase the temperature between the electrodes to 88°C, it is necessary to increase the voltage to 40 V. In this case, the maximum temperature will increase to 235°C, the coefficient of unevenness is 2.67, which is unacceptable. Therefore, we can conclude that it is inappropriate to use an insulating plate with a thickness of 4–5 mm or more.

Table 1

Research results for dielectric thicknesses of 2, 3, and 4 mm

Dielectric thickness, mm	Voltage, V	Hemostasis width, mm	Average electrode movement speed, mm/s	Depth of hemostasis, mm
2	20	4.4	29.3	0.8
2	25	5.4	36	1.5
2	30	6.4	42.6	1.6
3	20	6.9	16.4	1.8
3	25	7.9	18.1	2.2
3	30	8.6	20.5	2.8
4	20	7	16.6	1.5
4	25	8.6	20.5	2
4	30	9.7	23.1	2.5

The results of our studies are given in Table 1.

The maximum average tool movement speed of 42.6 mm is achieved with an insulating dielectric thickness of 2 mm and a voltage of 30 V. In this case, the dimensions of the hemostasis zone are close to the average values. The minimum movement speed of 16.6 mm/s will be with a dielectric thickness of 4 mm and a voltage of 20 V. The dimensions of the hemostasis zone are close to the average values. Therefore, the optimal dielectric thickness is close to 2–3 mm. An instrument with a dielectric thickness of 2 mm is used to obtain the same hemostasis conditions throughout the wound surface. A tool with a dielectric thickness of 3 mm is used to obtain the maximum depth of the hemostasis area. It does not make sense to use an instrument with an insulating plate thickness of more than 4–5 mm due to uneven temperature distribution.

6. Discussion of results based on investigating an electrosurgical instrument with a split electrode

The ANSYS simulation produced the distributions of the electric voltage (Fig. 3), its gradient (Fig. 4), the Joule heat density (Fig. 5), and temperature (Fig. 6, 8–12) throughout the heating time. Unlike [8, 9], in which the temperature is measured at individual points, our simulation gives the distribution over the entire study volume not only of the temperature but also of the voltage, its gradient, and other information. It is impossible to obtain such information by experimental methods due to the small size of the study area and the speed of the processes.

During the operation of the instrument, the tissue can heat up to high temperatures (Fig. 7). For tissue, a temperature of more than 100°C will lead to necrosis. In order to avoid thermal damage, it is necessary to turn off the voltage or move the instrument when a dangerous temperature is reached. If the hemostasis zone is within the surgeon's visibility, s/he manually adjusts the speed of the instrument movement. If the hemostasis zone is hidden from the surgeon, in contrast to [20, 21], it is necessary to use systems for automatic control of tissue impedance [23]. Initially, the impedance drops and reaches a minimum value. Further heating causes coagulation and an increase in the relative impedance value. When the relative impedance value becomes greater than 1.3–1.5, the voltage begins to decrease, preventing excessive heating of the tissue.

In [3–5, 11–14], the results of using the instrument in clinical practice without information about the modes were reported. Engineering analysis supplements information about clinical studies, significantly accelerates the design of electrosurgical instruments, significantly reduces the need for experiments on experimental animals, saves money and time.

Certain limitations in this study is the assumption about constant tissue parameters during the coagulation process, the assumption about a homogeneous tissue structure, and the dependence of coagulation only on temperature, and not on temperature and its duration. The disadvantage of the study is modeling the first stage of work only, when the initial temperature of the instrument is 36.6°C. At subsequent stages, the instrument gradually heats up, which accelerates tissue heating and its coagulation.

Another disadvantage of our work is the failure to take into account the influence of the skin effect on the displacement of current to the surface of electrodes. When advancing the topic, it is planned to eliminate these limitations and shortcomings. Engineering analyses of split electrode instruments used in other areas of surgery should also be conducted to improve them.

It would be desirable in further studies to verify the results of engineering analysis engaging experimental animals with different modifications of instruments and sensors. This requires appropriate resources and financial support.

7. Conclusions

1. The shape and dimensions of the biological tissue coagulation area depend on dielectric thickness, voltage, and exposure time. The qualitative characteristics of the coagulation process are also influenced by these parameters. At a dielectric thickness of 2–3 mm, the coagulation area has a semicircular shape. With a dielectric thickness of 4 mm or greater, the maximum heat density is at the electrodes. The coagulation depth varies from 0.8 to 2.8 mm and the coagulation width from 4.4 to 9.7 mm, depending on dielectric thickness and voltage.

2. The optimal dielectric thickness, according to the quantitative indicators obtained in the study, is approximately 2–3 mm. The average speed of movement of the tool is from 16.4 mm/s to 42.6 mm/s.

Conflicts of interest

The authors declare that they have no conflicts of interest in relation to the current study, including financial, personal, authorship, or any other, that could affect the study and the results reported in this paper.

Funding

The study was conducted without financial support.

Data availability

All data are available in the main text of the manuscript.

Use of artificial intelligence

The authors confirm that they did not use artificial intelligence technologies when creating the current work.

Authors' contributions

Alexei Lebedev: Conceptualization, Methodology, Software; **Vladyslav Shlykov:** Validation, Formal analysis, Investigation; **Andrii Dubko:** Resources, Data Curation, Writing – original draft; **Stanislav Popov:** Writing – review & editing, Visualization.

References

1. Krivtsun, I., Kvasnytskyi, V., Maksimov, S. (2023). Welding in medicine applications. Welding of Metallic Materials, 399–429. https://doi.org/10.1016/b978-0-323-90552-7.00008-0
2. Lebedev, A. V., Dubko, A. G. (2020). Use of Electric Welding of Living Tissues in Surgery (review). Biomedical Engineering, 54 (1), 73–78. https://doi.org/10.1007/s10527-020-09977-3
3. Kosakivskyi, A., Kosakivska, I. (2023). Vykorystannia elektrozvariuvalnoi tekhnolohiyi pry zakhvoriuvanniakh limfohlotkovoho kiltsia u ditei. Kyiv: NUOZ Ukrainy imeni P.L. Shupyka, 248. Available at: https://www.nuozu.edu.ua/n/p/11052-monohrafiia-vykorystannia-elektrozvariuvalnoi-tekhnolohii-pry-zakhvoriuvanniakh-limfohlotkovoho-kiltsia-u-ditei#gsc.tab=0
4. Umanets, N., Pasyechnikova, N. V., Naumenko, V. A., Henrich, P. B. (2014). High-frequency electric welding: a novel method for improved immediate chorioretinal adhesion in vitreoretinal surgery. Graefe's Archive for Clinical and Experimental Ophthalmology, 252 (11), 1697–1703. https://doi.org/10.1007/s00417-014-2709-0
5. Umanets, N. (2016). High-frequency electric welding of biological tissues versus diode laser photocoagulation as intraoperative retinopexy in vitrectomy for rhegmatogenous retinal detachment. Oftalmologicheskii Zhurnal, 63 (5), 14–17. https://doi.org/10.31288/oftalmolzh201651417
6. Umanets, N., Pasyechnikova, N., Naumenko, V., Maletskyi, A., Chabotarev, E., Pukhlik, E. (2016). Endoresection of choroidal melanoma using high-frequency electric welding of biological tissues. Oftalmologicheskii Zhurnal, 62 (4), 11–14. https://doi.org/10.31288/oftalmolzh201641114
7. Krestianov, M. Y., Kunkin, D. D., Savytska, I. M., Heilenko, O. A., Kalashnikov, V. A. (2025). Effects of bio-welding on small intestine tissues in automatic mode using artificial intelligence algorithms. The Ukrainian Journal of Clinical Surgery, 92(2), 55–59. https://doi.org/10.26779/2786-832x.2025.2.55
8. Muzychenko, P. F., Chernyak, V. A., Savosko, S. I., Lankin, Yu. N., Karpenko, K. K., Dubenko, D. E. et al. (2021). Morphological Assessment of Vascular Anastomoses Performed Using High Frequency Electric Welding. International Journal of Morphology, 39 (4), 1183–1189. https://doi.org/10.4067/s0717-95022021000401183
9. Yin, L., Zhu, C., Xu, J., Zhao, H., Qiu, J., Wang, H., Liu, K. (2022). Dynamic Impedance Analysis of Intestinal Anastomosis during High-Frequency Electric Field Welding Process. Sensors, 22 (11), 4101. https://doi.org/10.3390/s22114101
10. Dziuba, I., Bondarenko, Y., Koroliuk, T., Dubko, A., Stepenko, S., Bondarenko, O. (2024). Experimental Determination of Biological Tissue Impedance for Electrosurgical Process. 2024 IEEE 6th International Conference on Modern Electrical and Energy System (MEES), 1–7. https://doi.org/10.1109/mees64070.2024.11405055
11. Molotkovets, V. Yu., Medvediev, V. V., Korsak, A. V., Chaikovsky, Yu. B., Marynsky, G. S., Tsymbaliuk, V. I. (2020). Restoration of the Integrity of a Transected Peripheral Nerve with the Use of an Electric Welding Technology. Neurophysiology, 52 (1), 31–42. https://doi.org/10.1007/s11062-020-09848-3
12. Zabolotnyi, D., Kvasha, O. (2023). Biophysical evaluation of the effectiveness of high-frequency bipolar electric welding for closing defects in the dura mater in frontal sinus tumours with intracranial spread. Bulletin of Medical and Biological Research, 17 (3), 16–24. https://doi.org/10.61751/bmbr.2706-6290.2023.3.16

13. Zabolotnyi, D., Kvasha, O. (2023). Experimental development of the method of seamless connection of the dura mater using high-frequency bipolar electric welding and substantiation of its greater tightness, compared to the traditional method of connection using suture material. Grail of Science, 31, 447–458. https://doi.org/10.36074/grail-of-science.15.09.2023.72
14. Zabolotnyi, D., Kvasha, O. (2023). Bipolar high-frequency electric welding in radical resection of frontal sinus tumors. Carcinogenesis, 44 (2), 175–181. https://doi.org/10.1093/carcin/bgad018
15. Fomin, P. D., Vasylchenko, V. A., Oparin, S. O., Feleshtynskyi, Ya. P., Chvertko, N. A. (2020). Pat. na korysnu model No. 146869 UA. Elektrokhirurhichnyi instrument dlia endoskopichnykh maloinvazyvnykh operatyvnykh vtruchan v abdominalniy khirurhiyi. No. u202004787; zaiavl. 27.07.2020, opubl. 31.03.2021. Available at: https://sis.nipo.gov.ua/uk/search/detail/1585870/
16. Dubko, A. G., Chvertko, N. A., Lebedev, O. V. (2021). Electrosurgical instrument for minimally invasive interventions in abdominal surgery. Biomedical Engineering and Technology, 6, 11–18. https://doi.org/10.20535/2617-8974.2021.6.244548
17. Wang, H., Yang, X., Madeniyeti, N., Qiu, J., Zhu, C., Yin, L., Liu, K. (2022). Temperature Distribution of Vessel Tissue by High Frequency Electric Welding with Combination Optical Measure and Simulation. Biosensors, 12 (4), 209. https://doi.org/10.3390/bios12040209
18. Paton, B. Ye., Lebediev, V. K., Lebediev, O. V. et al. (2007). Pat. No. 29797 UA. Instrument dlia bipoliarnoi vysokochastotnoi koahuliatsiyi zhyvykh miakykh tkanyn tvaryn i liudyny. No. u200711208; declareted: 10.10.2007, published: 25.01.2008. Available at: https://sis.nipo.gov.ua/uk/search/detail/312265/
19. Lebediev, V. K., Lebediev, O. V., Vasylchenko, V.A., Paton, B. Ye., Bushtedt, Yu. P. (2007). Pat. No. 32967 UA. Elektroinstrument dlia bipoliarnoi vysokochastotnoi koahuliatsii zhyvykh miakykh tkanyn tvaryn i liudyny. № u200800573; declareted: 10.10.2007, declareted: 10.06.2008. Available at: https://sis.nipo.gov.ua/uk/search/detail/315453/
20. Kosakivska, I. A. (2020). Surgical Treatment of Chronic Tonsillitis. Family Medicine, 1-2, 121–124. https://doi.org/10.30841/2307-5112.1-2.2020.20460
21. Linchevskyy, O., Makarov, A., Getman, V. (2010). Lung sealing using the tissue-welding technology in spontaneous pneumothorax. European Journal of Cardio-Thoracic Surgery, 37 (5), 1126–1128. https://doi.org/10.1016/j.ejcts.2009.11.017
22. Popovic, Z., Popovic, B. (1999). Introductory Electromagnetics. Prentice Hall, 548. Available at: https://www.scribd.com/doc/92105971/Introductory-Electromagnetics-Z-Popovic-B-Popovic
23. Paton, B. E., Lebedev, V. K., Vorona, D. S. et al. (2003). Pat. No. US20040068304 A1. Bonding of soft biological tissues by passing high freouency electric current therethrough. No. 10/673,358; declareted: 26.09.2003. Available at: https://patentimages.storage.googleapis.com/11/cd/7f/59bce5b450ff56/US20040068304A1.pdf